Physico-Chemical Properties of New Liquid Crystals Incorporating a Lactone Ring

Yuki Morita [a] , Takeyasu Tasaka [a] , Remuto Yamaguchi [a] , Hiroaki Okamoto [a] & Shunsuke Takenaka [a]

[a] Department of Advanced Materials and Science, Faculty of Engineering, Yamaguchi University, Tokiwadai, Ube, Yamaguchi, Japan

Version of record first published: 31 Aug 2006

PLEASE SCROLL DOWN FOR ARTICLE

Taylor & Francis
Taylor & Francis Group

Physico-Chemical Properties of New Liquid Crystals Incorporating a Lactone Ring

Yuki Morita
Takeyasu Tasaka
Remuto Yamaguchi
Hiroaki Okamoto
Shunsuke Takenaka
Department of Advanced Materials and Science, Faculty of Engineering, Yamaguchi University, Tokiwadai, Ube, Yamaguchi, Japan

Synthesis and physico-chemical properties of 4-alkoxyphenyl and 4-alkoxybiphenyl-4'-yl 2H-pyran-2-one-5-carboxylates, 2H-chromen-2-one-6-yl 4-alkoxybenzoates and 4-alkoxybiphenyl-4'-carboxylates, and 2H-chromen-2-one-7-yl 4-alkoxybenzoates and 4-alkoxybiphenyl-4'-carboxylates are described. Terminal 2H-pyran-2-one and chromen-2-one cores are effective in enhancing liquid crystalline properties. The layer structure was examined by a small angle X-ray measurement, and the results are discussed in terms of the molecular structure. The polar effect of the terminal lactone group is recognized in the thermal properties and the layer structure of smectic A (SmA) phase.

INTRODUCTION

It is well known that terminal polar groups such as a cyano or a nitro group play important roles in determining thermal properties of liquid crystal (LC) molecules. Especially, the polar interactions cause a complex polymesomorphism involving plural smectic A (SmA), C phases, and also reentrant nematic one [1].

Y. Morita et al.
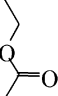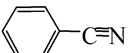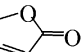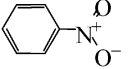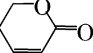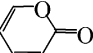
	μ_{obs}	μ_{cal}		μ_{obs}	μ_{cal}
(ethyl acetate)	1.78 [2]	1.87	(benzonitrile)	4.05 [6]	3.34
(furanone)	4.62 [3]	4.75	(nitrobenzene)	3.96 [7]	5.24
(dihydropyranone)	5.08 [4]	5.25			
(pyranone)		5.44 [5]			

FIGURE 1 Dipole moments of ester and lactone compounds. Dipole moments (μ_{cal}, D) were estimated by a semi-empirical molecular orbital calculation (MOPAC2000).

Although cyano and nitro groups have been considered to be the typical example of a polar substituent, in practice, a lactone ring has larger dipole moment than those, as shown in Figure 1.

An ester group intrinsically should have a large dipole moment due to electronic distortion on two oxygen atoms. However, the dipole moment of ethyl acetate, for example, is not so high (1.78 D). Cancellation of the electronic distribution in the conformation should be responsible for the reduction. A semi-empirical molecular orbital calculation (MOPAC2000) predicts the reduction of dipole moment (1.87 D). In contrast, dipole moments of cyclic esters (lactones) such as furan-2(5H)-one and 5,6-dihydropyran-2-one are much larger than those of benzonitrile and nitrobenzene. These facts predict that the related lactone, 2H-pyran-2-one also has a large dipole moment.

We are interested in the polar effect of 2H-pyran-2-one and the related lactone, 2H-chromen-2-one on LC properties, since MO calculation predicts that these have a planer structure being preferable in displaying LC properties and large dipole moment, 5.44 and 4.82 D, respectively. In this paper, we describe preparation and LC properties of new compounds **1**~**3**. The smectic layer structure will be discussed in terms of physical properties of the molecules. The chemical structures are illustrated in Figure 2.

EXPERIMENTAL

Materials

Compounds **1a**-n and **1b**-n were prepared by a conventional esterification (DCC method in THF) with 2H-pyran-2-one-5-carboxylic acid and 4-alkoxyphenols or 4-alkoxybiphenyl-4'-ols. **2a**-n and **2b**-n were
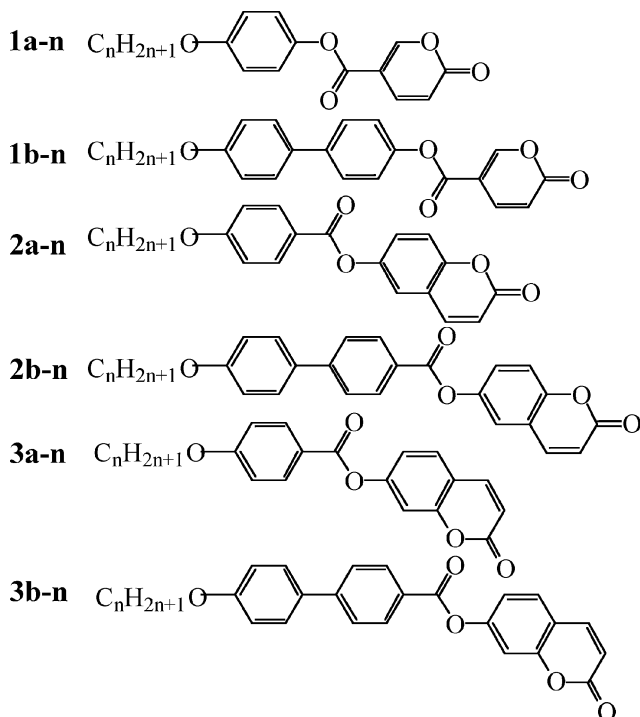
FIGURE 2 Chemical structure of **1**∼**3**.

prepared by a similar esterification of 6-hydroxy-2*H*-chromen-2-one and the acids. 6-Hydroxy-2*H*-chromen-2-one was prepared according to the synthetic scheme in Figure 3, while another way has been reported [8].

Compounds **3a**-n and **3b**-n were prepared by a similar esterification with 7-hydroxy-2*H*-chromen-2-one and 4-alkoxybenzoic acids or 4-alkoxybiphenyl-4′-carboxylic acids.

Methods

The transition temperatures and latent heats were determined using a Seiko SSC-5200 DSC. Mesophases were characterized using a Nikon POH polarizing microscope fitted with a Mettler thermo-control system (FP-900).

X-ray diffraction experiments for the smectic phases were performed using a Rigaku-denki RINT 2200 diffractometer, where CuKα ($\lambda = 1.541\,\text{Å}$) was used as an X-ray source. Temperature was controlled using a Rigaku PTC-20A thermo-controller.

Y. Morita et al.

mp=147 °C
^{1}H NMR (CDCl$_3$)
δ=3.80 (3H, s), 3.85 (3H, s), 6.52 (1H, d, J=16.2 Hz), 6.85 (1H, d, J=9.2 Hz), 6.94 (1H, dd, J=9.2, 3.0 Hz), 7.06 (1H, d, J= 3.0 Hz), 8.06 (1H, d, J=16.2 Hz), and 11.5 (1H, br s, OH) ppm.
IR (KBr disc) ν=1680 and 2839 cm^{-1}

mp=215 °C
^{1}H NMR (DMSO-d6)
δ=6.58 (1H, d, *J*=9.6 Hz), 7.09-7.12 (3H, m), 7.31 (1H, J=9.5 Hz), 8.04 (1H, d, *J*=9.6 Hz), and 9.83 (1H, br s, OH) ppm.
IR (KBr disc) ν=1676 and 3205 cm^{-1}
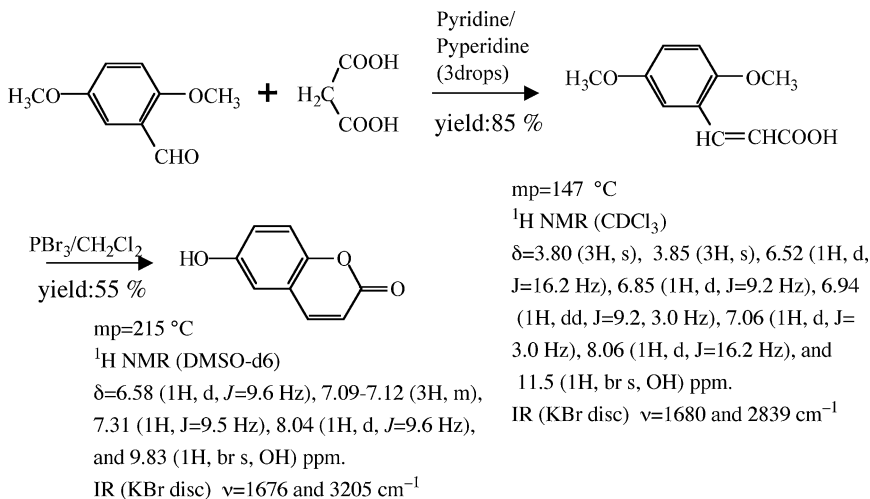
FIGURE 3 Synthetic scheme of 6-hydroxy-2*H*-chromen-2-one.

RESULTS AND DISCUSSION

Thermal Properties

Transition temperatures of **1a**-n and **1b**-n are summarized in Table 1.

Considering the fact that 4-alkoxyphenyl 4-cyanobenzoates exhibit nematic (N) phase and SmA one which commences from the octyloxy homologue, and the N-isotropic (I) transition temperatures for the

TABLE 1 Transition Temperatures of **1a**-n and **1b**-n

Compounds	n	C	SmA$_{low}$	SmA	N	I
1a	5	• 68	–	–	–	•
	6	• 76	–	–	–	•
	7	• 72	–	(• 48)	–	•
	8	• 80	–	(• 59)	–	•
	9	• 72	–	(• 65)	–	•
	10	• 74	–	(• 69)	–	•
1b	4	• 151	(• 142)	–	• 203	•
	5	• 145	(• 130)	–	• 197	•
	6	• 148	(• 129)	• 172	• 190	•
	7	• 144	(• 120)	• 174	• 189	•

C, SmA, N, and I indicate crystal, smectic A, nematic, and isotropic phases, respectively. Parentheses represent a monotropic transition temperature.

homologues are ca. 90℃, the terminal lactone core for **1a**-n may be less favorable than benzonitrile one for the appearance of the N phase [9].

Compounds **1b**-4∼**1b**-7 exhibit N and SmA phases, and **1b**-6 and **1b**-7 exhibit two kinds of SmA phases, namely SmA$_{low}$ and SmA in Table 1. The latent heats for the SmA$_{low}$–SmA transition were so small that the phase transition temperature was only determined by a microscopic observation, where a quick and notable change of texture was observed near the phase transition point.

Transition temperatures of **2a**-n and **2b**-n are summarized in Table 2.

Considering the fact that N–I transition temperatures for 2-cyano-naphthalene-6-yl 4-alkoxybenzoates are up to 150℃, the 2*H*-chromen-2-one core may be less favorable than the 2-cyanonaphthalene one in displaying LC properties [10].

Similar tendency is observed in **2b**-4∼**2b**-7, where N–I transition temperatures are 30∼40℃ lower than those of 2-cyanonaphthalene-6-yl 4-alkoxybiphenyl-4′-carboxylates [10].

Transition temperatures of **3a**-n and **3b**-n are summarized in Table 3.

Compounds **3b**-4 and **3b**-5 instantaneously exhibit N phase on the cooling process. The bent geometry around the terminal position should be responsible for low N–I transition temperature.

The thermal properties of SmA phases were examined by binary phase diagrams, and the results are shown in Figures 4.

TABLE 2 Transition Temperatures for **2a**-n and **2b**-n

Compounds	n	C	SmA	N	I
2a	2	● 160	–	– [*]1	●
	3	● 102	–	(● 75)	●
	4	● 98	–	(● 78)	●
	5	● 88	–	(● 78)	●
	6	● 96	–	(● 80)[*]2	●
	7	● 101	–	(● 84)[*]2	●
	8	● 105	–	(● 88)[*]2	●
	9	● 104	(● 84)	–	●
	10	● 106	(● 95)	–	●
	12	● 108	● 108	–	●
2b	5	● 155	–	● 249	●
	6	● 149	–	● 240	●
	7	● 154	–	● 235	●
	8	● 151	● 208	● 232	●

[*]1 A schlierene texture was observed before recrystallization. [*]2 Transition temperatures were determined from binary phase diagrams, for example, in Figure 6a.

Y. Morita et al.

TABLE 3 Transition Temperatures for **3a**-n and **3b**-n

Compounds	n	C	N	I
3a	6	● 116	–	●
	8	● 112	–	●
	12	● 112	–	●
3b	4	● 209	(● 207)	●
	5	● 215	● *1	●

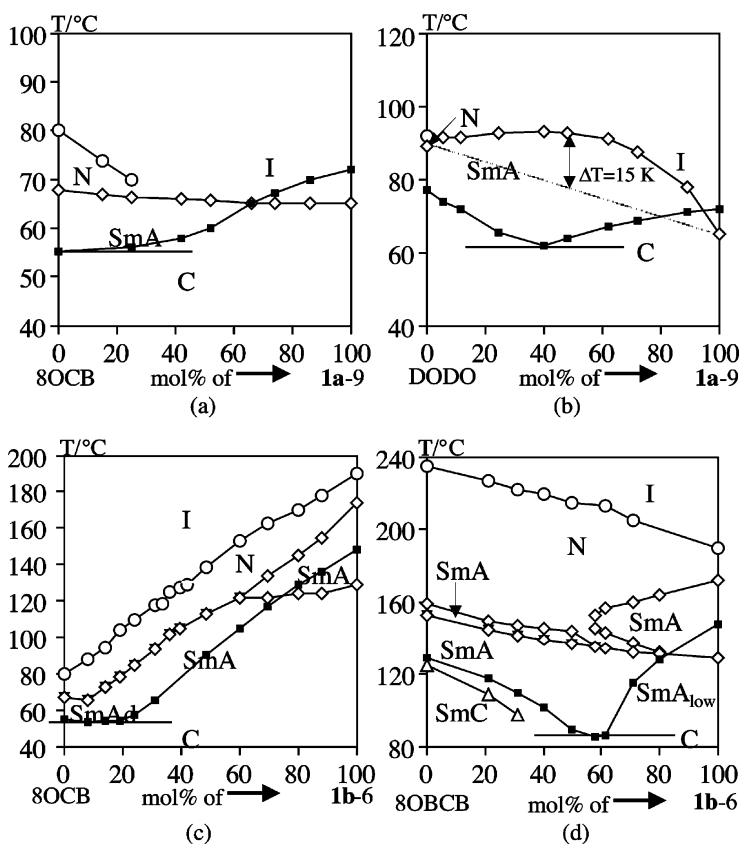*1 A schlierene texture was observed before recrystallization.

FIGURE 4 Binary phase diagrams for mixtures of: (a) 4-octyloxy-4′-cyano-biphenyl (8OCB) (on left) and **1a**-9 (on right), (b) 4-decyloxyphenyl 4-decyloxy-benzoate (DODO) and **1a**-9, (c) 8OCB and **1b**-6, and (d) 4-octyloxybiphenyl-4-yl 4-cyanobenzoate (8OBCB) and **1b**-6. Transitions below melting points were observed on the monotropic process.

For the mixture of 4-octyloxy-4′-cyanobiphenyl (8OCB) and **1a**-9 in Figure 4a, the SmA phase of **1a**-9 is miscible with that of 8OCB, and the SmA–N (I) transition temperature shows a linear correlation against mol% of each component. However, the N phase of 8OCB hides under the SmA phase around 30 mol% of **1a**-9, suggesting that the N–I transition temperature of **1a**-9 is low compared with the SmA–I one.

In the binary phase diagram for the mixture of 4-decyloxyphenyl 4-decyloxybenzoate (DODO) and **1a**-9 (Fig. 4b), the SmA–I transition temperature shows an upward convexity (ca. 15 K around the center of the diagram). The peculiar feature is frequently observed in polar and non-polar LC mixtures, and molecular interactions and the rearrangement of each component are supposed to be responsible for the enhancement [11].

Compounds **1b**-6 and **1b**-7 exhibit two kinds of SmA phases and experience the SmA_{low}–SmA transition. The miscible relation between SmA phases of **1b**-6 and 8OCB was examined, and the results are shown in Figure 4c. Thereby, the SmA phase of 8OCB has been assigned to the SmA_d modification, where the layer spacing is 1.5 times of the fully extended molecular length [12]. Although the SmA–N transition temperature varies linearly through the mixture, another SmA–SmA transition should occur in the range between 0 and 20 mol% of 8OCB.

4-Octyloxybiphenyl-4′-yl 4-cyanobenzoate (8OBCB) should have a similar geometrical and electrostatic nature to **1b**-n and show a phase transition sequence of SmC–SmA–SmA–N–I type [13]. For the mixture of 8OBCB and **1b**-6 in Figure 4d, both SmA phases at the lower temperature region are miscible each other, and the SmA–SmA(N) transition temperature shows a linear correlation to mol% of each component, indicating that low SmA phases of both components have similar physical properties and a monolayer arrangement (SmA_1). On the other hand, the SmA phases at the higher temperature region are discontinuous in the diagram, and reentrant N phase is exhibited around their boundary. Therefore, both SmA phases should be classified into "SmA_d" modification.

XRD Measurement

The layer structure of SmA phase was further characterized by a small angle X-ray diffraction method.

The observed layer spacing (d_{obs}) of **1a**-n is plotted against temperature and the hydrocarbon chain length (n) in Figures 5a and 5b, respectively.
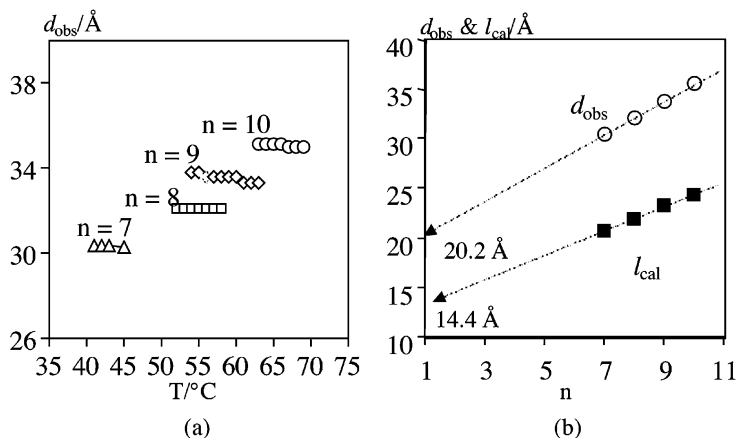
FIGURE 5 Plots of: (a) layer spacings (d_{obs}) vs. temperature for **1a**-n, and (b) layer spacings (d_{obs}, ○) and calculated molecular length (l_{cal}, ◇) vs. n.

The d_{obs} of **1a**-9 varies in the range between 33.3 Å at 63°C and 33.8 Å at 54°C in Figure 5a, so that 33.7 Å was used as the mean value in Figure 5b. The layer spacings for the other homologues in Figure 5a are almost independent of temperature. The d_{obs} is plotted against n in Figure 5b, and apparently has a linear correlation with n within the range of n = 7∼10, and a linear curve fitting method for the plot gives d_{obs}(Å) = 1.70n + 18.5, meaning that the extrapolated layer spacing of **1a**-1 is 20.2 Å, and the d_{obs} for n = 7∼10 homologues increases by 1.70 Å/n.

In order to correlate these results with molecular parameters, the molecular shape and length were estimated by a semi-empirical molecular orbital calculation (MOPAC2000). The MO calculation predicts that the alkoxy chain extends linearly beside the aromatic ring in the most stable conformation, so that the calculated molecular length (l_{cal}) is proportional to n, as shown in Figure 5b. The linear curve fitting method gives l_{cal} (Å) = 1.21n + 13.2, indicating that the molecular length is 14.4 Å for **1a**-1 and increases by 1.21 Å/n on ascending the homologues.

A molecular arrangement model in SmA phase is illustrated in Figure 6a, where molecules are voluntarily put in an x–y coordinate, and the x-axis is supposed to be a smectic layer.

In such conditions, the d_{obs} is given by $l_{core}\cos\theta_{core} + l_{chain}\cos\theta_{chain}$, where l_{core} and l_{chain} are longitudinal lengths of LC core and hydrocarbon chain, respectively. l_{core} and l_{chain} can be obtained easily and exactly by the MO calculation. Of course, the plot of l_{cal} values vs.
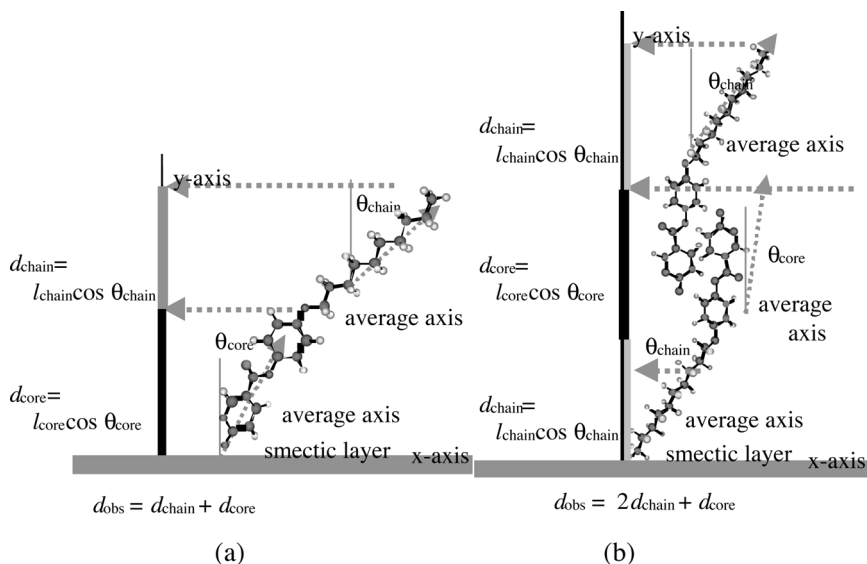
FIGURE 6 Molecular arrangement models in SmA phase for **1a**-10. (a) monolayer, (b) partially bilayer.

n gives a straight line, as shown in Figure 5b. A similar treatment of X-ray data has been tried by several authors [14–16].

For the model in Figure 6a, increment of the layer spacing should be $1.25\,\text{Å}/n$ ($1.51\cos55.5$, C−C bond length $= 1.51\,\text{Å}$, C−C−C bond angle $= 111°$), when $\theta_{chain} = 0$, that is, the hydrocarbon chain arranges orthogonal to the smectic layer. The large slope ($1.70\,\text{Å}/n$) for the d_{obs} of **1a**-n in Figure 5b suggests that an interdigitation of molecules occurs within the smectic layer. In fact, the d_{obs} is far long from the longest molecular lengths.

Based on these results, a modified model is postulated and illustrated in Figure 6b, where molecules interdigitate within the smectic layer.

For the model, the LC core is supposed to arrange orthogonal to the smectic layer, and the l_{core} is set to $20.2\,\text{Å}$ on the analogy of the d_{obs} of **1a**-1, and corresponds to 1.40 times of calculated core length ($14.4\,\text{Å}$). In such conditions, the reflected length of the hydrocarbon chain on the y-axis is given by $2d_{chain}$(i.e., $2l_{chain}\cos\theta_{chain}$), and the d_{obs} is given by $2d_{chain} + d_{core}$. From these equations, we can calculate the tilt angle (θ_{chain}) of the hydrocarbon chain to the smectic layer, giving $47°$ for **1a**-n in Figure 5b.

A similar feature is observed for the plots of **1b**-n. The plots of the d_{obs} vs. T and n are shown in Figures 7a and 7b, respectively.
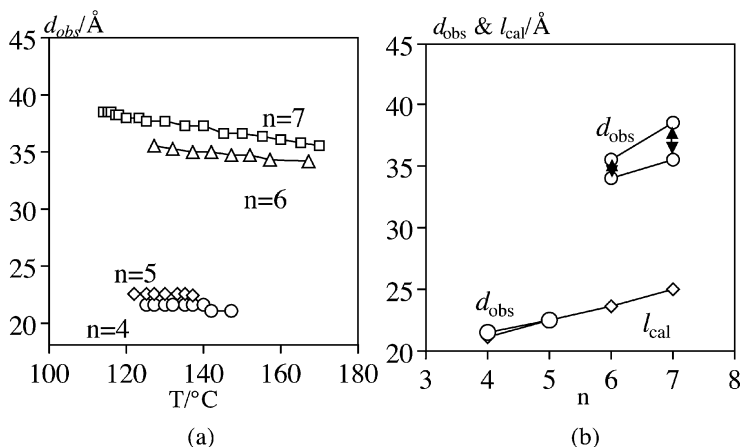
Y. Morita et al.

FIGURE 7 Plots of: (a) layer spacings (d_{obs}) vs. temperature for **1b**-n, (b) layer spacings (d_{obs}, O) and calculated molecular lengths (l_{cal}, ◇) vs. n. Bold lines indicate the temperature dependency of layer spacings.

In Figure 7a the d_{obs} values of **1b**-4 and **1b**-5 are almost independent of temperature. In contrast, those of **1b**-6 and **1b**-7 are considerably large compared with **1b**-4 and **1b**-5, and in addition, the temperature dependency is notable. The notable temperature dependency may be concerned with the fact that these homologues have two kinds of SmA phases, and experience the SmA_{low}–SmA transition at ca. 130°C. The layer spacing of the SmA_{low} phase, unfortunately, could not be measured due to recrystallization.

In Figure 7b the d_{obs} values of **1b**-4 (21.4 Å) and **1b**-5 (22.5 Å) are in good agreement with the l_{cal}s (21.2 and 22.6 Å, respectively), indicating that the SmA phase has a monolayer arrangement. Supposing that the plots of **1b**-6 and **1b**-7 show a straight line, the line is presented as $d_{obs}(Å) = 1.70n + 24.8$, where the extrapolated d_{obs} of **1b**-1 is 26.5 Å. On the other hand, the l_{cal} (Å) is given by $1.22n + 16.3$, where the molecular length for **1b**-1 is 17.5 Å. Considering the fact that the ratio of d_{obs} to l_{cal} is 1.51, the interdigitation also occurs in the SmA phase of **1b**-6 and the after homologues. Interestingly, the slope of 1.70 is similar to that of **1a**-n, so that the tilt angle of the alkoxy chain to the smectic layer may be ca. 45°.

Although both **2a**-10 and **2a**-12 exhibit a monotropic SmA phase, the X-ray measurement for the former was unsuccessful because of recrystallization. The d_{obs} of **2a**-12 is 37.9 and 37.8 Å at 98 and 104°C, respectively, corresponding to 1.3 times of l_{cal} (29.4 Å).

For **2b**-n, SmA phase was observed from the octyloxy homologue. The d_{obs} of the SmA phase for **2b**-8 is 38.1, 37.7, and 37.5 Å at 177, 165, and 157°C, respectively, indicating that the layer spacing is almost independent of temperature. The d_{obs} corresponds to 1.25 times of the molecular length of **2b**-8 (28.4 Å).

Interestingly, X-ray profiles for the N phase of **2b**-7 also show a wide and intense reflection peak at $2\theta = 2.46$, 2.48, and 2.48° at 183, 168, and 153°C, respectively, while the SmA phase could not be observed by microscopic and DSC measurements. These results suggest that cybotactic domains with the SmA layer structure are present in the N phase of **2b**-7.

Conclusively, polar interactions around the terminal lactone moieties are considered to play important roles in modification of the layer structure in SmA phase.

Dielectric Properties

The effect of the lactone group on dielectric properties has been reported in our previous paper, and it was clarified that the lactone moieties increase the positive dielectric anisotropy ($\Delta\varepsilon \sim 20$) [17,18].

CONCLUSIONS

2*H*-Pyran-2-one and 2*H*-chromen-2-one are a useful segment of LC molecules. The polar interaction around the lactone moieties causes of complex phase transition behavior in smectic A phases, where the layer spacing is $1 \sim 1.5$ times of the molecular length. These cores enhance the positive dielectric anisotropy.

REFERENCES

[1] Gray, G. W. & Goodby, J. W. (1984). *Smectic Liquid Crystals*, Heyden and Son Inc.,: Philadelphia, 134.
[2] Watson, H. E., Kane, G. P., & Ramaswamy, K. L. (1936). *Proc. Roy. Soc. A*, *156*, 137.
[3] Puchalik, M. (1950). *Acta Phys. Polon.*, *10*, 89.
[4] Sing, L. Y. (1987). *J. Mol. Structure*, *159*, 37.
[5] Brouckere, D. & Berthier, G. (1983). *Mol. Phys.*, *49*, 1417.
[6] Gloves, L. G. & Sugden, S. (1934). *J. Chem. Soc.*, 1094.
[7] Le Fevre, R. J. W. (1950). *Trans. Faraday Soc.*, *46*, 1.
[8] Sato, K., Inoue, S., Ozawa, K., Kobayashi, T., Ota, T., & Tazaki, M. (1987). *J. Chem. Soc., Perkin Trans.*, *1*, 1753.
[9] Goodby, J. W., Leslie, T. M., Cladis, P. E., & Finn, P. L. (1984). *Liquid Crystals and Ordered Fluids*, *4*, 89.
[10] Coates, D. & Gray, G. W. (1976). *Mol. Cryst. Liq. Cryst.*, *37*, 249.
[11] Kelker, H. & Hatz, R. (1980). *Handbook of Liquid Crystals*, Verlag Chemie: Weinheim, 340.

[12] Cladis, P. E. (1999). In: *Physical Properties of Liquid Crystals*, Demus, D., Goodby, J. W., Gray, G. W., Spiess, H.-W., & Vill, V. (Eds.), Wiley-Vch: Weinheim, 289.

[13] 4-Octyloxybiphenyl-4′-yl 4-cyanobenzoate (8OBCB) has a phase sequence of C·129·SmC·125·SmA·153·SmA·160·N·235·I (T/°C). The layer spacing of the SmA phase at high temperature region is 39.9 and 40.0 Å at 160 and 155°C, respectively, and those at low temperature region are 27.2 Å in the range between 151 and 125°C, and 27.5 Å at 120°C. Both reflection peaks co-exist in the temperature range between 140 and 160°C, and the relative intensity of both peaks notably varies without changing their positions. The layer spacings of 40.0 and 27.2 Å correspond to 1.48 and 1.0 times of the calculated molecular length (26.9 Å).

[14] Blumstein, A. & Patel, L. (1978). *Mol. Cryst. Liq. Cryst.*, *48*, 151.

[15] Ostrovskii, B. I., Tournilhac, F. G., Blinov, L. M., & Haase, W. (1995). *J. Phys. II France*, *5*, 979.

[16] Diele, S., Lose, D., Kruth, H., Pelzl, G., Guittard, F., & Cambon, A. (1996). *Liquid Crystals*, *21*, 603.

[17] Morita, Y., Tasaka, T., Kabu, K., Okamoto, H., & Takenaka, S. (2003). *IDW '03*, 217.

[18] Morita, Y., Tasaka, T., Kabu, K., Okamoto, H., Kasatani, K., & Takenaka, S. (2004). *Trans. Mater. Res. Soc. Jpn.*, *29*, 831.